# Two-Phase Convective Heat Transfer in Miniature Pipes Under Normal and Microgravity Conditions

**Chidambaram Narayanan**

**Djamel Lakehal**[1]
e-mail: lakehal@ascomp.ch

ASCOMP GmbH,
Technoparkstrasse 1,
8005 Zurich, Switzerland

*Detailed numerical simulations have been performed to study the effect of flow orientation with respect to gravity on two-phase flow heat transfer (without phase change) in small diameter pipes. The Nusselt number distribution shows that the bubbly, slug, and slug-train regimes transport as much as three to four times more heat from the tube wall to the bulk flow than pure water flow. The flow blockage effect of the inclusions results in a circulating liquid flow superimposed on the mean flow. For upflow, the breakup into bubbles/slugs occurs earlier and at a higher frequency. The average Nusselt numbers are not significantly affected by the flow orientation with respect to gravity. A mechanistic heat transfer model based on frequency and length scale of inclusions is also presented.* [DOI: 10.1115/1.2909076]

*Keywords: two phase, heat transfer, miniature pipes*

## 1 Introduction

Experimental research on thermal flow in miniature pipes has so far centered on three issues: (i) flow regime map and transition, (ii) confinement effects, and (iii) characterization of heat transfer in the presence of phase change. Convective two-phase flow heat transfer without phase change has surprisingly been absent from the list of priorities. The experiment of Monde and Mitsutake [1] is one of the rare exceptions. Computational studies are rarer, except the recent contribution of Ua-Arayaporn et al. [2], who investigated convective two-phase flow heat transfer in small tubes in a small periodic box rather than in an elongated tube, as done in the companion paper by the current authors [3]. Together with our earlier study [3], the present communication sets up a debate on the following question: Is it practically meaningful to resort to convective two-phase flow heat transfer without phase change as an alternative for select microcooling applications?

In this contribution, we compare new simulation results for two-phase flow subject to gravity (upflow and downflow) to the earlier data obtained at zero gravity [3]. The focus here is on the role played by flow regimes and associated blockage/confinement effects in controlling heat transfer.

## 2 Modeling and Simulation

The incompressible Navier–Stokes equations within the one-fluid formalism are used in this study. The level set method is used for interface tracking. Temperature was treated as a passive scalar, such that it is merely transported by the flow. The CMFD code TransAT© developed at ASCOMP is a finite-volume multiblock structured-mesh code solving the one-fluid Navier–Stokes equations. Details of the equations and numerical methods used are available in Ref. [3].

## 3 Two-Phase Flow Regimes and Heat Transport

**3.1 Numerical Setup.** The data used as reference are from the experiments by Chen et al. [4]. In their experiments, air-water flow was pumped at various flow rates in a closed loop into 1 mm and 1.5 mm diameter pipes. Five flow regimes were investigated in horizontal pipes: Bubbly, slug, slug train, churn, and annular. The simulations were performed under axisymmetric conditions for single- and two-phase flows for zero-gravity, down-flow, and up-flow configurations. The small diameter and reasonably high velocities (around 1 m/s) result in high Froude numbers of $\approx 100$, justifying the comparison between the zero-gravity simulations and horizontal flow in the experiments.

The pipe wall was set to a constant temperature $T_w = 340$ K, and the inflow to $T_{\text{in}} = 300$ K. The inlet flow conditions were extracted from the experiment. The phase inflow velocities and corresponding void fractions $\alpha$ are listed in Table 1; the void fractions were set by adjusting the inlet area.

For typical values of velocity = 1.11 m/s, liquid viscosity $= 10^{-3}$ kg/m s, surface tension coefficient = 0.072 N/m, and liquid density = 1000 kg/m$^3$, one obtains a Capillary number $\approx 0.0154$, a Weber number $\approx 17$, and a Reynolds number $\approx 1110$. This suggests that the resulting flow will be dominated by the interplay between inertia and surface tension.

Grid and domain size sensitivity studies revealed that a domain extension of at least 40 diameters is necessary for the two-phase flows to establish a periodic pattern around the inclusions. Grid independence required the domain to be covered by $900 \times 30$ cells (half the diameter). Note that the slug-train case is not described in detail here.

**3.2 Flow Regimes.** Figure 1(*a*) compares the zero-gravity (central panel) bubbly flow patterns to down-(upper panel) and up-flow (lower panel) conditions. The gas jet breaks at $x/D = 4$ when surface tension effects exceed the inertia. Individual bubbles are then periodically released. Gravity has an impact on the breakup time/length, with breakup happening the earliest for the up-flow case, followed by zero gravity and downflow (see Table 2). This is because the effect of gravity counters inertia when the flow is against gravity, thus making surface tension more dominant.

As discussed by the authors before [3], the breakup into slugs (Fig. 1(*b*)) takes place further downstream as compared to the bubbly flow because of the higher void fraction requiring a larger amplitude of the instability wave to develop before breakup. The effect of gravity is stronger for slug flow as compared to bubbly flow. The slug breakup happens slightly earlier for upflow, which results in a higher breakup frequency. Figure 1(*b*) also reveals the strong interaction between the slug and the wall, the proximity shown later to be responsible for substantial heat transport down to the core-flow region.

**3.3 Nusselt Number.** In order to quantify the increase in heat transfer in two-phase flow, the Nusselt number (see Ref. [3] for details) variation along the wall is presented in Figs. 2(*a*) and 2(*b*) for bubbly and slug flows, respectively, and compared to their equivalent single-phase flow distributions. The comparison reveals a substantial increase in the heat transfer rate with increasing inclusion length scale, denoted in Table 2 as $L_{\text{GB}}$. For the bubbly flow, an average Nusselt number of $\approx 10.7$ is obtained for all the three cases with different orientations relative to gravity. For the slug flow, an average Nusselt number of $\approx 15$ is obtained. In this case, a discernible trend is present with respect to gravity orientation. The down-flow case has a 4% higher $\text{Nu}_{\text{avg}}$ as compared to

[1]Corresponding author.

Contributed by the Heat Transfer Division of ASME for publication in the JOURNAL OF HEAT TRANSFER. Manuscript received April 2, 2007; final manuscript received October 3, 2007; published online May 16, 2008. Review conducted by Louis C. Chow.

**Table 1 Inflow velocity and void fraction conditions**

| Case study | $\alpha$ | $U_G$ (m/s) | $U_L$ (m/s) | Domain size |
|---|---|---|---|---|
| Water | 0.0 | 0 | 1.11 | $1\times 70\ D$ |
| Bubbly | 0.205 | 0.66 | 1.11 | $1\times 40\ D$ |
| Slug | 0.376 | 0.66 | 1.11 | $1\times 40\ D$ |
| Slug-train | 0.480 | 1.57 | 1.11 | $1\times 40\ D$ |

**Table 2 Average Nusselt numbers, time, and length scales**

| Case | $\mathrm{Nu}_{\mathrm{mean}}$ | Freq. (Hz) | $L_{\mathrm{GB}}/D$ | $\mathrm{Re}_{\mathrm{LS}}$ |
|---|---|---|---|---|
| Water (single phase) | 3.67 | 0.0 | 0.0 | — |
| Bubbly (downflow) | 10.76 | 632 | 0.8 | 505.6 |
| Bubbly (zero gravity) | 10.69 | 669 | 0.8 | 535.2 |
| Bubbly (upflow) | 10.72 | 727 | 0.8 | 581.6 |
| Slug (downflow) | 15.44 | 391 | 1.8 | 703.8 |
| Slug (zero gravity) | 14.81 | 414 | 1.8 | 745.2 |
| Slug (upflow) | 14.72 | 439 | 1.8 | 790.2 |
| Slug-train 1 | 15.61 | 519 | 2.7 | 1401 |
| Slug-train 2 | 17.20 | 350 | 5.14 | 1799 |

the zero-gravity case (which in turn has a 1% higher value than upflow). For the slug-train flows (not presented here), average Nusselt numbers of $\approx$15.6 and 17 were obtained. These numbers imply an overall enhancement in heat transfer by a factor between 3 and 4 compared to single-phase flow. This purely hydrodynamic effect should be taken into consideration in conditions where phase change results in similar two-phase flow regimes [5].

A closer view of the Nusselt number variation (Fig. 3) reveals that it has a very coherent variation around each inclusion. For the bubbly flow, the Nusselt number smoothly goes through a maximum at the center of the bubble where the liquid layer is squeezed. For the slug flow, the maximum value of the Nusselt number occurs at the rear end of the slug where the gap between the interface and the wall is very small (see Fig. 4(*c*)). Values as high as 32 can be observed. Orientation with respect to gravity plays a role in shifting the location of breakup upstream for the up-flow case, which results in a larger breakup frequency. The Nusselt numbers obtained are of similar magnitudes to those obtained by others [2,1].

**3.4 Defect-Flow Analysis.** In order to clarify the mechanism enhancing heat transfer, the flow field has been decomposed into the sum of the single-phase flow and a perturbation flow superimposed on top of it (induced by the presence of inclusions), i.e., $U=U_{sp}+U_p$. Results of this flow decomposition are presented below in Fig. 4 for bubbly and slug flows; the snapshots are taken at approximately 26 diameters from the inlet in a periodic cell around an inclusion. For each flow regime, the top figures show the total velocity vectors at four stations in the periodic cell and the bottom figures show the perturbation flow components. The perturbation flow field is of a circulating nature around the inclusion such that near the wall, the shear is increased as compared to a single-phase profile. This additional shear created by the perturbation flow field is responsible for increasing the heat transfer rate in two-phase flow.

## 4 Mechanistic Heat Transfer Modeling

For practical applications, it is desirable to have a simple mechanistic model for the heat transfer coefficient. A simple anal-

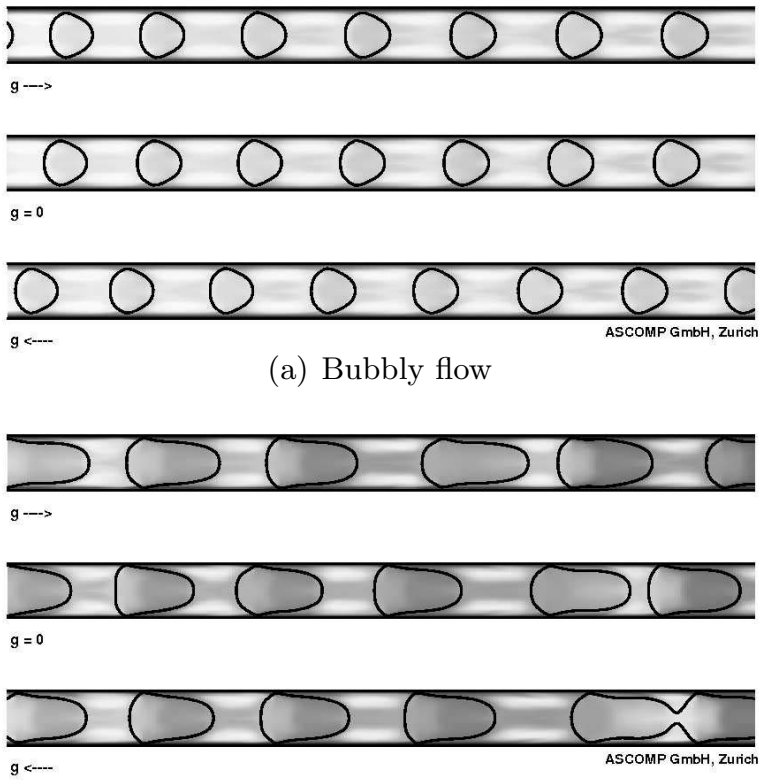


**Fig. 1 Flow evolution under normal- and microgravity conditions. Domain: 18–32 *D*. Scale: Higher temperature corresponds to darker shade.**

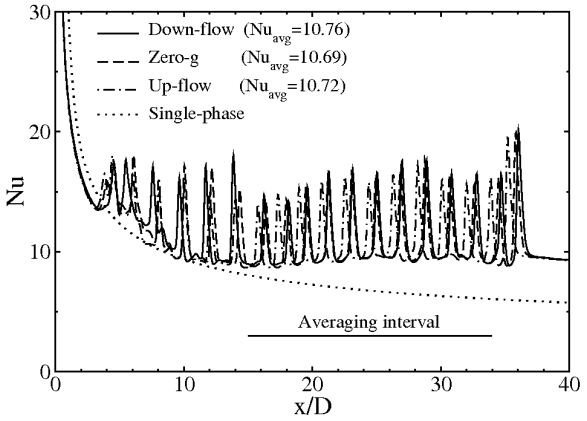


(a) Bubbly flow

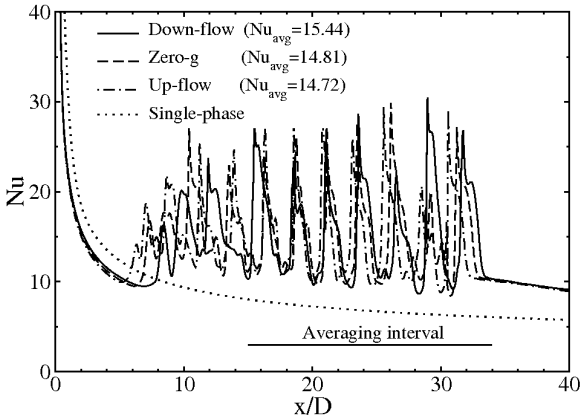


(b) Slug flow

**Fig. 2 Nusselt number distribution along the axis under normal- and microgravity conditions**

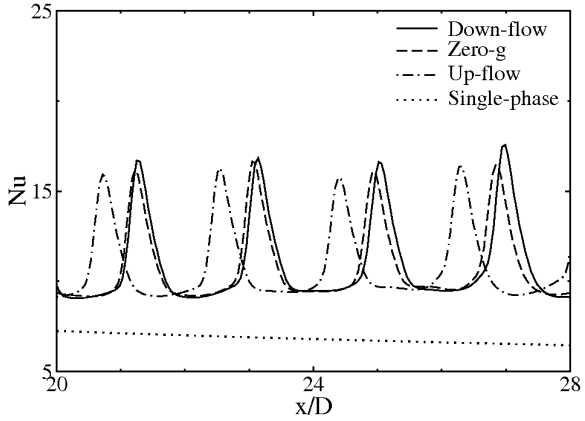


(a) Bubbly flow

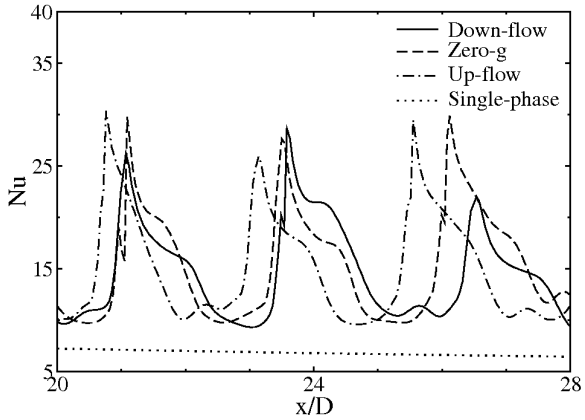


(b) Slug flow

**Fig. 3 Detailed view of Nusselt number distribution under normal- and microgravity conditions**

ogy with turbulent flow has been successfully proposed [3], where it was postulated that the passage of individual bubbles and slugs may act as fluid structures or eddies washing out the wall-adjacent layer, thereby increasing the temperature gradient at the wall. This is the spirit of surface renewal theory of Higbie [6].

Using the Dittus–Boelter [7] expression for heat transfer in turbulent pipe flows, the Nusselt number may be expressed as follows:

$$\mathrm{Nu} \approx \mathrm{Nu}_w + C\,\mathrm{Pr}_L^{0.4}\,\mathrm{Re}_{\mathrm{LS}}^{4/5} \tag{1}$$

where $\mathrm{Nu}_w$ is the value for fully developed single-phase flow (equal to 3.67 for constant wall temperature and 4.36 for constant wall heat flux), $C$ is a model constant, and $\mathrm{Re}_{\mathrm{LS}}$ is the liquid slug Reynolds number defined based on the pipe diameter $D$ and the velocity scale of the inclusions $V_{\mathrm{GB}}$. Therefore, $\mathrm{Re}_{\mathrm{LS}}=DV_{\mathrm{GB}}/\nu L$, where $V_{\mathrm{GB}}=L_{\mathrm{GB}}/\tau$ and $\tau$ is the time scale of bubble/slug passage.

The frequency of bubble/slug detachment together with the inclusion characteristic length scale $L_{\mathrm{GB}}$ is reported in Table 2. These would be better estimates of the flow time and length scales, rather than simply the superficial inflow velocities and void fraction. Bubbles detach at a higher frequency as compared to the slug and slug train, but have a smaller streamwise length. This dichotomy should be taken into account in the mechanistic modeling of heat transfer.

The best fit to the computational data is obtained for a model constant $C=0.022$, as shown in Fig. 5, which is of the same order of magnitude as the original Dittus–Boelter correlation ($C=0.023$). The frequency of breakup and passage of inclusions is systematically affected by the orientation of the flow with respect to gravity. Up-flow case has a higher frequency as compared to zero gravity, which in turn has a higher frequency than the down-flow case. Since the inclusion length scales $L_{\mathrm{GB}}$ are not affected by gravity, the above correlation holds for both down- and up-flow cases.

This model can be used to determine the Nusselt number in similar situations involving well defined gas inclusions such as bubbles, and slugs evolving in microfluidic devices, where $L>1$ mm, and for $\mathrm{Pr}>1$ liquids. As shown in Fig. 5, the proposed model fits remarkably well the simulated Nusselt number data for the range of flow topologies. This is a new valuable result for practical applications.

## 5 Pressure Drop

The effect of gravity on the pressure drop is intuitive. Pressure drop is higher in the case of upflow as compared to zero-gravity and down-flow cases in that order. Interestingly, it is observed that while the bubbly flow (Fig. 6(*a*)) has a lower pressure drop than the single-phase water flow (except the up-flow case), the slug flow (Fig. 6(*b*)) has a 14–15% larger pressure drop than the single-phase flow.

The factors affecting pressure drop are the mass flow rates, which reduce with increasing void fraction, and the inclusion-induced wall shear, which increases with void fraction. In the bubbly flow regime, the reduction in the mass flow rate has a higher impact than the bubble-induced increase in the shear, resulting in a lower pressure drop. In the slug flow (and the slug-

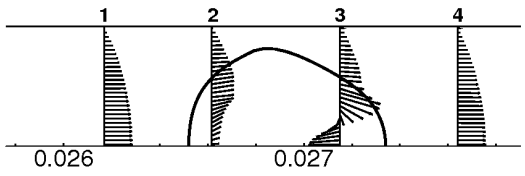


(a) Flow over bubble and stations

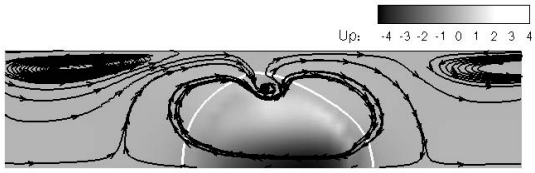


(b) Defect flow over bubble

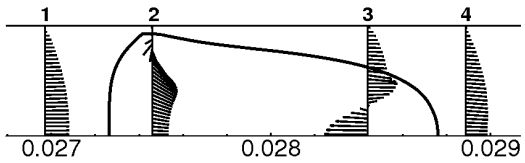


(c) Flow over slug and stations

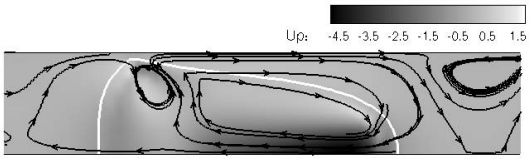


(d) Defect flow over slug

**Fig. 4 Total and defect flow fields**

train flow), the mass flow rate is even lower but the shear stress is significantly larger in proportion, which explains the increase in pressure drop. Thus, an optimum condition could exist, which enhances heat transfer by a factor of 4 with no increase in pressure drop.

Note that in Fig. 6(*b*), the axial pressure profile for the down-flow case has a large downward shift. This particular instance has been chosen to show the effect of the breakup phenomenon, as shown in Fig. 7. During the process of necking, a large pressure

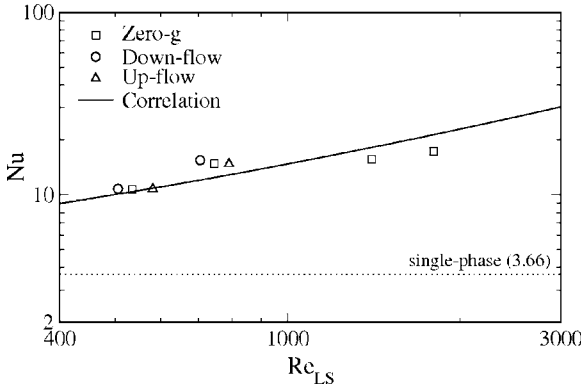


**Fig. 5 Nusselt number correlation as a function of Reynolds number**

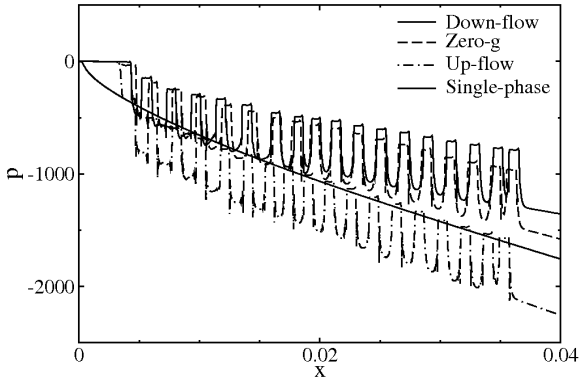


(a) Bubbly flow

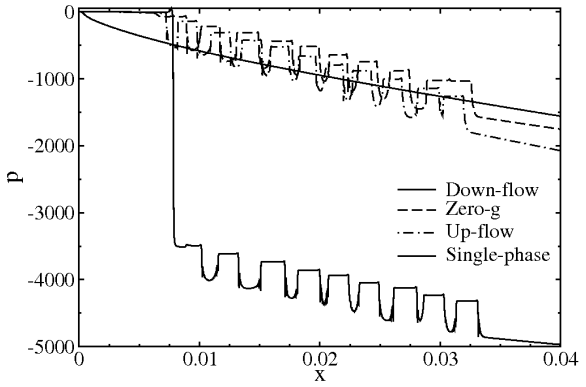


(b) Slug flow

**Fig. 6 Pressure variation along the pipe for normal- and microgravity conditions**

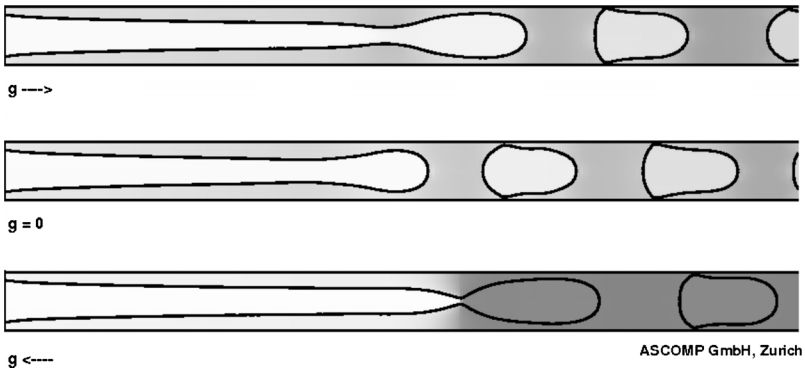


**Fig. 7 Slug breakup under normal- and microgravity conditions**

drop is created across the neck due to gas flow acceleration, which produces this downward shift in pressure. The relevant point here is that in designing a two-phase system, these pressure pulses will have to be taken into account, even though the average pressure drop would be similar to single-phase flow.

## 6 Conclusions

Overall, the heat removal rate in two-phase flow is significantly higher than in single phase. The additional circulating flow induced by the presence of bubbles and slugs is shown to substantially increase the wall shear and in turn heat transfer. The average Nusselt number distribution shows that the bubbly and slug patterns transport three to four times more heat from the tube wall to the bulk flow than the single-phase water flow. The heat transfer results are only marginally affected by gravity, even though there is a noticeable effect on the breakup frequency. From an engineering standpoint, the present results may be helpful in designing intelligent flow control systems. The simple correlation proposed is meant to be used as a guideline for design purposes.

## Acknowledgment

This work has been granted by the European Space Agency (ESA) through the MAP research program MAP AO-1999-045. The authors are thankful to the Coordinators, Olivier Minster (ESA) and Professor Lounes Tadrist (University of Marseille) for their valuable comments.

## References

[1] Monde, M., and Mitsutake, Y., 1995, "Enhancement of Heat Transfer Due to Bubble Passing Through a Narrow Vertical Rectangular Channel," Heat Mass Transfer, **31**, pp. 77–82.
[2] Ua-Arayaporn, P., Fugakata, K., Kasagi, N., and Himeno, T., 2005, "Numerical Simulation of Gas-Liquid Two-Phase Convective Heat Transfer in a Microtube," *Proceedings of the ECI International Conference on Heat Transfer and Fluid Flow in Microscale*, Castelvecchio Pascoli, Italy, Sept. 25–30.
[3] Lakehal, D., Larrignon, G., and Narayanan, C., 2007, "Computational Heat Transfer and Two-Phase Flow Topology in Miniature Tube," Microfluid. Nanofluid., **4**, pp. 261–271.
[4] Chen, W. L., Twu, M. C., and Pan, C., 2002, "Gas-Liquid Two-Phase Flow in Microchannels," Int. J. Multiphase Flow, **28**, pp. 1235–1247.
[5] Thome, J. R., Dupont, V., and Jacobi, A. M., 2004, "Heat Transfer Model for Evaporation in Microchannels, Part I: Presentation of the Model," Int. J. Heat Mass Transfer, **47**, pp. 3375–3385.
[6] Higbie, R., 1935, "The Rate of Absorption of Pure Gas Into a Still Liquid During Short Period of Exposure," Trans. Am. Inst. Chem. Eng., **31**, pp. 365–388.
[7] Dittus, F. W., and Boelter, L. M. K., 1930, "Heat Transfer in Automobile Radiators of the Tubular Type," Univ. Calif. Publ. Eng., **2**(13), pp. 443–461.